# Hall effect in the marginal Fermi liquid regime of high-$T_c$ superconductors

Elihu Abrahams
*Center for Materials Theory, Serin Physics Laboratory, Rutgers University, Piscataway, New Jersey 08854-8019, USA*

C. M. Varma
*Bell Laboratories, Lucent Technologies Murray Hill, New Jersey 07974, USA*

(Received 8 May 2003; published 4 September 2003)

The detailed derivation of a theory for transport in quasi-two-dimensional metals, with small-angle elastic scattering and angle-independent inelastic scattering is presented. The transport equation is solved for a model Fermi surface representing a typical cuprate superconductor. Using the small-angle elastic and the inelastic scattering rates deduced from angle-resolved photoemission experiments, good quantitative agreement with the observed anomalous temperature dependence of the Hall angle in *optimally* doped cuprates is obtained, while the resistivity remains linear in temperature. The theory is also extended to the frequency-dependent complex Hall angle.

DOI: 10.1103/PhysRevB.68.094502 PACS number(s): 74.20.Mn, 74.25.Fy

## I. INTRODUCTION

Soon after the discovery of high-temperature superconductivity in the cuprate compounds, it was found that all the transport properties for compositions near those for the maximum $T_c$ have anomalous temperature and/or frequency dependence, in contrast to what is expected for Landau Fermi liquids. Most of the anomalies, in resistivity and optical conductivity, in the frequency dependence of Raman intensity, in the tunneling spectra, and in the temperature dependence of the copper nuclear relaxation could be understood by the ''marginal Fermi liquid'' (MFL) phenomenology.[1] Within MFL, scale-invariant fluctuations in both the charge and magnetic sectors are assumed to have the form

$$\begin{aligned} \mathrm{Im}\,\chi(\mathbf{q},\omega,T) &= -N_0(\omega/T), \qquad \omega \ll T \\ &= -N_0(\mathrm{sgn}\,\omega), \quad T \ll \omega \ll \omega_c \end{aligned} \tag{1.1}$$

characteristic of a quantum critical point. $\omega$ is the frequency and $\mathbf{q}$ the momentum of the fluctuations, $N_0$ is the density of energy states per unit volume and $\omega_c$ is a high-frequency cutoff. At long wavelengths this form is observed directly in Raman scattering.[2] A principal prediction[1] from this hypothesis is that at low energies ($\omega \ll T$), the inelastic part of the single-particle relaxation rate has the MFL form $\lambda T$ with coefficient $\lambda$ having negligible momentum dependence either along or perpendicular to the Fermi surface. This form has been confirmed in angle-resolved photoemission (ARPES) experiments[3] and leads directly to the observed linear temperature dependence of the resistivity.

However, the temperature dependence of anomalies in the normal state Hall effect and magnetoresistance could not be understood by the MFL hypothesis alone. For example, for a situation near optimal doping, where the resistivity is linear in temperature, the expectation is that the cotangent of the Hall angle ($\sigma^{xx}/\sigma^{xy}$) should also be linear. Experiment shows it to be more nearly quadratic. This left open the possibility that essential new physics near optimum doping may not be captured by the MFL scenario. In this paper we show that the temperature dependence of the Hall angle may be understood quantitatively by a proper application of transport theory using the measured single-particle relaxation rates.

The single-particle self energy $\Sigma(\mathbf{k},\omega,T)$ is measurable in ARPES experiments.[3,4] As stated above, within MFL, the prediction is that the inelastic part of $\Sigma$ is $\mathbf{k}$ independent and of the MFL form,[1] proportional to $\omega$ for $\omega \gg T$ and to $T$ for $T \gg \omega$. ARPES experiments[3] do find the inelastic part of this form but find in addition an elastic part that varies in magnitude around the Fermi surface. Thus, as explained in detail earlier,[4] on the Fermi surface ($\omega = 0$), the experimentally measured self-energy consists of the MFL part $\lambda T$ and an anisotropic $T$-independent elastic part:

$$\mathrm{Im}\,\Sigma(\mathbf{k},T) = \lambda T + \gamma(\hat{\mathbf{k}}), \tag{1.2}$$

According to experiment, $\gamma(\hat{\mathbf{k}})$ increases by about a factor 4 to 5 going from the $(\pi,\pi)$ to the $(\pi,0)$ direction along the Fermi surface.[4] A crucial point is that even at its minimum value, it is more than an order of magnitude larger than the transport scattering rate due to impurities obtained by extrapolating the normal state resistivity to $T=0$. As argued in Ref. 4, such behavior arises if $\gamma(\hat{\mathbf{k}})$ comes from small-angle impurity scattering. We discuss this point further in Sec. VII.

In a previous communication,[5] we described, for high-$T_c$ superconductors, how Eq. (1.1) can be used in a Boltzmann equation analysis to account for observed anomalies[6–11] in the Hall effect. We performed a calculation (p. 4655 of Ref. 1) using a simple Fermi surface in order to give an example of how a new contribution[12] could dominate the conventional result and thus account for experimental observations. However, it was pointed out to us by Yakovenko[13] that we erred in the form we chose to parametrize $\gamma(\hat{\mathbf{k}})$.[14] The purposes of this paper are to give a more complete solution of the Boltzmann equation, correct the above error, and to present a model calculation that illustrates how, with a proper parametrization and a reasonable choice of parameters, the presence of the anisotropic impurity scattering together with

 

other anisotropies can account for the observed behavior of the Hall angle.[6–11] Further, we generalize our results to the complex Hall angle at finite frequencies, which has been recently measured.[15]

A point about the experimental results needs stressing. In many presentations of the data, for example Refs. 9 and 10, single-temperature noninteger power-law fits to the Hall number or the Hall angle have been made, with varying success, while integer power law fits[6] do not usually faithfully represent the data. There is no physical reason to expect integer power-law behavior, and our analysis shows quite generally that the solution of the Boltzmann equation can give a sum of contributions with different temperature dependences. In particular, it is usually found[9,10] that a temperature power law with a power less than 2 can fit the data for the cotangent of the Hall angle. As we show here, this is indistinguishable from the ratio of terms each of which is a sum of contributions with different temperature dependences.

Our results have two significant conclusions. First, anisotropies, especially in the scattering rate, introduce corrections to the calculation of magnetotransport properties so that conventional results such as $R_H=(nec)^{-1}$ or $\tan\theta_H=\omega_c\tau_{tr}$ are not in general valid.[16] Second, the fact that the Hall effect in the cuprates can be understood within transport theory, with only the measured single-particle relaxation rate, the measured resistivity, and Fermi surface quantities as inputs, implies that no new physics is involved other than what leads to the behavior of those quantities. We conclude that the MFL, which gives the experimentally observed temperature dependence of the relaxation rate, is sufficient to account for all the anomalous magnetotransport near optimal doping. This point of view is reinforced by recent frequency-dependent complex Hall effect measurements,[15] whose results are consistent with the analysis presented here, as discussed in Sec. IV.

## II. TRANSPORT EQUATION

At long wavelengths and low frequencies the derivation of Boltzmann equation relies only on conservation laws and is valid whether the system is a Fermi liquid or not. Therefore we start with the linearized Boltzmann equation for the deviation $g(\mathbf{k},t)$ of the momentum distribution function from its equilibrium value $f(\mathbf{k})$ in the presence of uniform static electric and magnetic fields,

$$\frac{\partial g_{\mathbf{k}}}{\partial t}+e\mathbf{E}\cdot\mathbf{v}_{\mathbf{k}}\frac{\partial f}{\partial\epsilon_{\mathbf{k}}}+\frac{e}{\hbar c}(\mathbf{v}_{\mathbf{k}}\times\mathbf{B})\cdot\boldsymbol{\nabla}_{\mathbf{k}}g_{\mathbf{k}}=C_{\mathbf{k}}. \tag{2.1}$$

Here $C_{\mathbf{k}}$ is the collision operator. The solution to this equation for the stationary case ($\omega=0$) is given by[18]

$$g(\mathbf{k})=e\hbar\sum_{\mathbf{k}'}A^{-1}_{\mathbf{k},\mathbf{k}'}\left[\mathbf{E}\cdot\mathbf{v}_{\mathbf{k}'}\left(-\frac{\partial f}{\partial\epsilon_{\mathbf{k}'}}\right)\right], \tag{2.2}$$

where

$$A_{\mathbf{k},\mathbf{k}'}=\hbar\left[\frac{1}{\tau(\mathbf{k})}+\frac{e}{\hbar c}\mathbf{v}_{\mathbf{k}}\times\mathbf{B}\cdot\boldsymbol{\nabla}_{\mathbf{k}}\right]\delta_{\mathbf{k},\mathbf{k}'}-C_{\mathbf{k},\mathbf{k}'}. \tag{2.3}$$

Here $C_{\mathbf{k},\mathbf{k}'}$ is the ''scattering-in'' term in the collision operator for the Boltzmann equation and $\hbar/\tau(\mathbf{k})=\Sigma_{\mathbf{k}'}C_{\mathbf{k},\mathbf{k}'}$, is the ''scattering-out'' term equal to the single-particle relaxation rate. It is evident that the distribution $g(\mathbf{k})$ is not only determined by the energy of the state $\mathbf{k}$ but also by the anisotropy of the scattering. The distribution is depleted in directions of large net scattering and augmented in directions of small net scattering.

We calculate the conductivities using the single-particle scattering rate of Eq. (1.2). The conductivity tensor is

$$\sigma^{\mu\nu}=\frac{e^2\hbar}{\Omega}\sum_{\mathbf{k},\mathbf{k}'}v_{\mu,\mathbf{k}}A^{-1}_{\mathbf{k},\mathbf{k}'}v_{\nu,\mathbf{k}'}\left(-\frac{\partial f}{\partial\epsilon_{\mathbf{k}'}}\right), \tag{2.4}$$

where $\Omega$ is the sample (taken to be a plane) area. We expand $A^{-1}$ from Eq. (2.2) in powers of $\mathbf{B}$:[17]

$$A^{-1}=\mathcal{T}-(e/c)\mathcal{T}(\mathbf{v}\times\mathbf{B}\cdot\boldsymbol{\nabla})\mathcal{T}+(e/c)^2\mathcal{T}(\mathbf{v}\times\mathbf{B}\cdot\boldsymbol{\nabla})\mathcal{T}(\mathbf{v}\times\mathbf{B}\cdot\boldsymbol{\nabla})\mathcal{T}, \tag{2.5}$$

where [from Eq. (2.12) of Ref. 17]

$$\mathcal{T}_{\mathbf{k},\mathbf{k}'}=\frac{1}{\hbar}\left[\tau_{\mathbf{k}}\delta_{\mathbf{k},\mathbf{k}'}+\sum_{\mathbf{k}''}\tau_{\mathbf{k}}C_{\mathbf{k},\mathbf{k}''}\mathcal{T}_{\mathbf{k}'',\mathbf{k}'}\right]. \tag{2.6}$$

The first term in $A^{-1}$ gives the longitudinal conductivity, the second the Hall conductivity $\sigma^{xy}$, and the magnetoconductivity may be calculated from the third term.

As discussed above, the $\tau_{\mathbf{k}}$ is the MFL scattering plus the angle-dependent impurity piece:

$$1/\tau_{\mathbf{k}}=1/\tau_M+1/\tau_i(\hat{\mathbf{k}}). \tag{2.7}$$

Our approach to solving Eq. (2.5) is to take advantage of the properties of $1/\tau_M$ and $1/\tau_i$. The kernel $C$ in Eq. (2.6) comprises the vertex corrections for the various scattering mechanisms. Within the MFL regime, the $1/\tau_M$ is an $s$-wave scattering process so the MFL interaction does not appear in $C$. That leaves

$$C_{\mathbf{k},\mathbf{k}'}=2\pi\delta(\epsilon_{\mathbf{k}}-\epsilon_{\mathbf{k}'})|u_i(\theta,\theta')|^2, \tag{2.8}$$

where, e.g., $\theta$ is the angle of $\hat{\mathbf{k}}$ along the Fermi surface. We have argued[5,4] that the impurity scattering matrix element $u_i(\theta,\theta')$ involves scattering through small angles only. This property allows an expansion of the right-hand side of Eq. (2.6) in powers of a ''small-angle scattering parameter,'' $\theta_c$, which can itself be a function of $\theta$. We illustrate such an expansion for the calculation of $1/\tau_i$:

$$\frac{1}{\tau_i}(\theta)=\frac{1}{\hbar}\sum_{\mathbf{k}'}|u_i(\theta,\theta')|^2\delta(\epsilon'-\epsilon)\approx\theta_c U(\theta,\theta)N(\theta)+\frac{\theta_c^3}{24}\left[\frac{d^2}{d\theta'^2}U(\theta,\theta')N(\theta')\right]_{\theta'=\theta}. \tag{2.9}$$

Here we have used

$$\sum_{\mathbf{k}} = \frac{1}{2\pi}\int d\epsilon \int N(\theta)d\theta, \quad N(\theta)=\frac{\Omega}{2\pi\hbar}\,\frac{dk_t/d\theta}{v(\theta)}. \tag{2.10}$$

$N(\theta)$ is the density of states per unit energy at the Fermi surface at angle $\theta$ and $v(\theta)$ is the Fermi velocity. $dk_t$ is an infinitesimal taken tangent to the Fermi surface at the angle $\theta$. We have abbreviated $|u_i(\theta,\theta')|^2$ by $U(\theta,\theta')$. We shall describe below how experiments show that $\theta_c$ is indeed sufficiently small to justify such an expansion.

### III. LONGITUDINAL CONDUCTIVITY

We begin by determining the longitudinal conductivity within the model. We first give the solution for a general Fermi surface and then specialize to a particular example to illustrate the results.

From Eqs. (2.4) and (2.5), we have

$$\sigma^{xx}=\frac{e^2\hbar}{\Omega}\sum_{\mathbf{k}\mathbf{k}'} v^x_{\mathbf{k}}\mathcal{T}_{\mathbf{k},\mathbf{k}'}v^x_{\mathbf{k}'}\left(-\frac{\partial f}{\partial\epsilon'}\right). \tag{3.1}$$

Define the vector $\mathbf{L}$ as

$$\mathbf{L}_{\mathbf{k}}=\sum_{\mathbf{k}'}\mathcal{T}(\mathbf{k},\mathbf{k}')(-\partial f/\partial\epsilon')\mathbf{v}_{\mathbf{k}'}, \tag{3.2}$$

so that

$$\sigma^{xx}=\frac{e^2\hbar}{\Omega}\sum_{\mathbf{k}} v^x_{\mathbf{k}}L^x_{\mathbf{k}}. \tag{3.3}$$

Using Eq. (2.6) in Eq. (3.2), we find the integral equation for $\mathbf{L}$:

$$\mathbf{L}_{\mathbf{k}}=\frac{\tau_{\mathbf{k}}}{\hbar}\left[\left(-\frac{\partial f}{\partial\epsilon}\right)v^x_{\mathbf{k}}+\sum_{\mathbf{k}''}C_{\mathbf{k},\mathbf{k}''}\mathbf{L}_{\mathbf{k}''}\right]. \tag{3.4}$$

As discussed earlier, $C$ contains only the small-angle scattering so that

$$\mathbf{L}_{\mathbf{k}}=\frac{\tau_{\mathbf{k}}}{\hbar}\left[\left(-\frac{\partial f}{\partial\epsilon}\right)\mathbf{v}_{\mathbf{k}}+\int d\theta' N(\theta')U(\theta,\theta')\mathbf{L}_{\mathbf{k}'}\right], \tag{3.5}$$

which, since $\mathbf{L}$ is restricted to the Fermi surface, can be rewritten as

$$\frac{\hbar}{\tau(\theta)}\mathbf{L}(\theta)=\left(-\frac{\partial f}{\partial\epsilon}\right)\mathbf{v}(\theta)+\frac{\hbar}{\tau_i(\theta)}\mathbf{L}(\theta) + \int d\theta' N(\theta')U(\theta,\theta')[\mathbf{L}(\theta')-\mathbf{L}(\theta)], \tag{3.6}$$

where $1/\tau_i=1/\tau-1/\tau_M$ is given in Eq. (2.9). Given the small-angle scattering restriction on $U(\theta,\theta')$, we expand the difference $\mathbf{L}(\theta')-\mathbf{L}(\theta)$ and find the differential equation (primes indicate derivatives with respect to $\theta$)

$$\mathbf{M}(\theta)=\mathbf{v}(\theta)+u(\theta)\mathbf{M}''(\theta)+2u'(\theta)\mathbf{M}'(\theta), \tag{3.7}$$

where

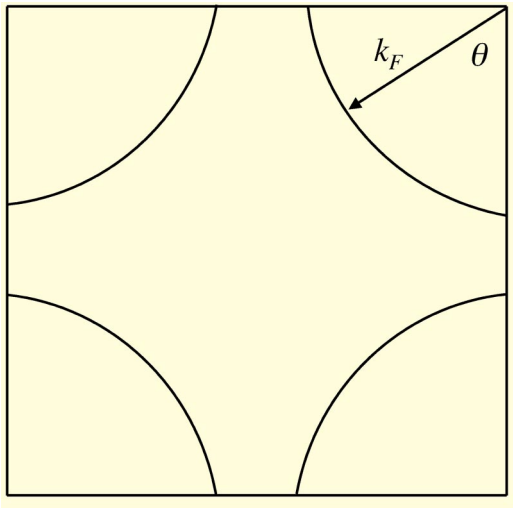


FIG. 1. Schematic Fermi surface.

$$\mathbf{M}(\theta)=\frac{\hbar}{\tau_M(-\partial f/\partial\epsilon)}\mathbf{L}(\theta), \tag{3.8}$$

and

$$u(\theta)=(\theta_c^3/24)(\tau_M/\hbar)N(\theta)U(\theta,\theta),$$
$$u'(\theta)=(\theta_c^3/24)(\tau_M/\hbar)\left[\frac{d}{d\theta'}N(\theta')U(\theta,\theta')\right]_{\theta'\to\theta}. \tag{3.9}$$

This differential equation can be solved for the components of $\mathbf{M}$, hence $\mathbf{L}$, once the $\theta$ dependences of $\mathbf{v}$, $u$, and $u'$ are known. This equation, which is basic to the evaluation of both the longitudinal and the Hall conductivities, is completely equivalent to Eq. (10) of Ref. 5. Although $u$ contains a small parameter, an iterative solution of Eq. (3.7), as in our previous work,[5] is not valid. We solve Eq. (3.7) exactly in this paper.

As we discussed previously,[5,14] the details of the anisotropies of the quantities entering the transport coefficients determine the magnitudes of the various contributions, in particular to $\sigma^{xy}$ in the presence of a magnetic field. The shape of the Fermi surface is especially important since it determines the size of the contribution to $\sigma^{xy}$ from the isotropic marginal Fermi liquid scattering rate $1/\tau_M$. In what follows, we take the anisotropy of the impurity scattering from ARPES data and we assume a simple form for the Fermi surface velocity.

A schematic of the Fermi surface is shown in Fig. 1, where the angular variable $\theta$ is shown. A general Fermi surface respecting the square symmetry of the $CuO_2$ layers must have Fermi velocities in the first quadrant of the form

$$v_x=\sum_n v_n\sin[(2n+1)\theta],$$
$$v_y=\sum_n v_n(-1)^n\cos[(2n+1)\theta]. \tag{3.10}$$

For our calculations we take a form for $\mathbf{v}(\theta)$, which is the simplest extension beyond the circular Fermi surface (similar to that shown in Fig. 1) consistent with Eq. (3.10). In the first quadrant,

$$v_x = v_0(\sin\theta + \rho\sin 3\theta),$$
$$v_y = v_0(\cos\theta - \rho\cos 3\theta). \tag{3.11}$$

For this choice for $\mathbf{v}(\theta)$, the density of states of Eq. (2.10) in all quadrants is

$$N(\theta) = \frac{\Omega}{2\pi\hbar}\frac{k_0(1-\rho)^{1/4}}{v_0(1-\rho\cos 4\theta)^{5/4}}, \tag{3.12}$$

where $k_0$ is the value of $k_F(\theta)$ at $\theta=0$. Thus, according to Eq. (3.3), $\sigma^{xx}$ is given by

$$\sigma^{xx} = \frac{e^2\tau_M(1-\rho)^{1/4}}{\pi^2\hbar}\,\frac{k_0}{v_0}\int_0^{\pi/2} d\theta \frac{v_x(\theta)M_x(\theta)}{(1-\rho\cos 4\theta)^{5/4}}. \tag{3.13}$$

## IV. HALL CONDUCTIVITY

For a magnetic field perpendicular to the $xy$ plane, $\mathbf{v}\times\mathbf{B}\cdot\boldsymbol{\nabla} = [\Omega/2\pi\hbar N(\theta)]B(\partial/\partial\theta)$ and from Eqs. (2.4) and (2.5),

$$\sigma^{xy} = \frac{e^3B}{2\pi c}\sum_{\mathbf{k},\mathbf{k}',\mathbf{k}_1} v^x_{\mathbf{k}}\frac{\mathcal{T}(\mathbf{k},\mathbf{k}_1)}{N(\theta_1)}\frac{d\mathcal{T}(\mathbf{k}_1,\mathbf{k}')}{d\theta_1}\left(-\frac{\partial f}{\partial\epsilon'}\right)v^y_{\mathbf{k}'}. \tag{4.1}$$

We rewrite this using Eq. (3.2):

$$\sigma^{xy} = \frac{e^3B}{2\pi c}\sum_{\mathbf{k},\mathbf{k}_1} v^x_{\mathbf{k}}\,\frac{\mathcal{T}(\mathbf{k},\mathbf{k}_1)}{N(\theta_1)}\frac{d}{d\theta_1}L^y_{\mathbf{k}_1}. \tag{4.2}$$

We define

$$\mathbf{K}_{\mathbf{k}} = \sum_{\mathbf{k}'}\mathcal{T}(\mathbf{k},\mathbf{k}')\frac{1}{N(\theta')}\frac{d}{d\theta'}\mathbf{L}_{\mathbf{k}'}, \tag{4.3}$$

so that

$$\sigma^{xy} = \frac{e^3B}{2\pi c}\sum_{\mathbf{k}} v^x_{\mathbf{k}}K^y_{\mathbf{k}}. \tag{4.4}$$

Using Eq. (3.4) in Eq. (4.3), we get an integral equation for $\mathbf{K}$:

$$\mathbf{K}_{\mathbf{k}} = \frac{\tau_{\mathbf{k}}}{\hbar}\left\{\frac{1}{N(\theta)}\mathbf{L}_{\mathbf{k}}{}' + \sum_{\mathbf{k}''} C_{\mathbf{k},\mathbf{k}''}\mathbf{K}_{\mathbf{k}''}\right\}$$
$$= \frac{\tau_{\mathbf{k}}}{\hbar}\left\{\frac{\mathbf{L}_{\mathbf{k}}{}'}{N(\theta)} + \int d\theta' N(\theta')U(\theta,\theta')\mathbf{K}(\theta')\right\}. \tag{4.5}$$

We proceed exactly as in the analysis for $\mathbf{L}$, Eqs. (3.4)–(3.9). For the required $K_y$, we find the differential equation

$$Z(\theta) = M_y'(\theta)(1-\rho\cos 4\theta)^{5/4} + u(\theta)Z''(\theta) + 2u'(\theta)Z'(\theta), \tag{4.6}$$

where $Z(\theta)$ determines $K_y(\theta)$ as

$$K_y(\theta) = \left(\frac{\tau_M}{\hbar}\right)^2\frac{2\pi}{\Omega}\frac{\hbar v_0}{k_0}\frac{1}{(1-\rho)^{1/4}}\left(-\frac{\partial f}{\partial\epsilon}\right)Z(\theta), \tag{4.7}$$

and $M_y$ is obtained as the solution of Eq. (3.7). As in that case, an iterative solution of Eq. (4.6) is not valid. Combining all our results into Eq. (4.4), we find

$$\sigma^{xy} = -\frac{e^3B}{\pi^2c}\left(\frac{\tau_M}{\hbar}\right)^2\int_0^{\pi/2}\frac{d\theta}{(1-\rho\cos 4\theta)^{5/4}}v_x(\theta)Z(\theta). \tag{4.8}$$

When there is no small-angle scattering, $M_y = v_y$ and $Z(\theta) = -v_0(\sin\theta - 3\rho\sin 3\theta)(1-\rho\cos 4\theta)^{5/4}$. In that case,

$$\sigma^{xy} \propto \int_0^{\pi/2} d\theta(\sin^2\theta - 3\rho^2\sin^2\theta), \tag{4.9}$$

which vanishes when $\rho = 1/\sqrt{3}$. This is the familiar result of the vanishing of $\sigma^{xy}$ when the Fermi surface consists of equal portions of positive and negative curvature. One sees that the anisotropic small-angle contributions, which have a leading contribution proportional to $\tau_M^3$, i.e., to $1/T^3$, do not vanish there.

## V. CHOICE OF PARAMETERS AND COMPARISON WITH EXPERIMENTS

We now describe the evaluation of the conductivities using experimental data from ARPES and from the longitudinal transport in zero magnetic field. The strategy is as follows. The anisotropies in the problem will be determined from the anisotropy of the impurity scattering $1/\tau_i(\theta) = 2\gamma(\hat{k})/\hbar$ as determined from ARPES. For simplicity, we shall let the density of states $N(\theta)$ be responsible for the anisotropy of $1/\tau_i$, and hence for the quantity $u(\theta)$ [see Eq. (3.9)]. The measured anisotropy of $1/\tau_i$ from the $(\pi,\pi)$ direction to the $(\pi,0)$ direction in the Brillouin zone then determines the velocity anisotropy parameter $\rho$ from Eqs. (2.9) and (3.12). These parametrizations give the correct behavior at the edges of the Brillouin zone. The small-angle parameter $\theta_c$ can then be found from the ''residual resistance'' ratio (RR) of the resistivity at $T_c$ to the extrapolated value at $T=0$. That is sufficient to determine the $T$ dependence of $\cot\theta_H = \sigma^{xx}/\sigma^{xy}$. The magnitude of $\cot\theta_H$ is then fixed by the effective mass $\hbar k_0/v_0$, which we leave as an adjustable parameter. It will be seen that the effective mass has a quite reasonable value.

The conductivities are given by Eqs. (3.13) and (4.8). The quantity $u$, which appears in the differential equations for $\mathbf{M}$ and $Z$, is defined as $u(\theta;T) = (\theta_c^2/24)\tau_M/\tau_i(\theta) = (\tau_M/\hbar)(\theta_c^3/24)N(\theta)U(\theta,\theta)$. The measured anisotropy[4] of $\gamma(\hat{\mathbf{k}}) = \hbar/2\tau_i$ is about 4.5. We assign this to $N(\theta)$, thus determining $\rho$ from Eq. (3.12) as $\rho = 0.54$. Therefore, we have

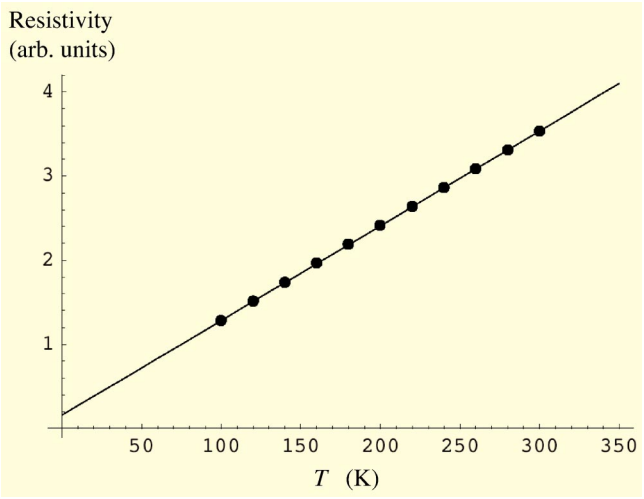


FIG. 2. Linear temperature fit to calculated resistivity (dots) from Eq. (4.8) for $\theta_c^2/24=0.0014$. The resistance ratio, $\rho(100)/\rho(0)$, is 8.

$$1/\tau_i(\theta)=(1/\tau_0)(1-\rho\cos 4\theta)^{-5/4},$$

$$u(\theta;T)=u_0(T)(1-\rho\cos 4\theta)^{-5/4}, \qquad (5.1)$$

$$\rho=0.54.$$

The quantity $u_0(T)=\tau_M(T)(\theta_c^2/24)/\tau_0$. $\tau_M(T)$ and $\tau_0$ may be determined from ARPES as described in Ref. 3. From ARPES, $\hbar/\tau_i\approx 0.24$ eV at $\theta=\pi/8$. So $\hbar/\tau_0=0.24$ eV. From the same source, $\hbar/\tau_M=0.015(T/100)$ eV, where $T$ is in kelvin. This determines $u_0$ as $u_0(T)=16(100/T)(\theta_c^2/24)$. The remaining parameter $u_0$, that is, $\theta_c$, is determined from the resistance ratio RR as follows.

The longitudinal resistivity in zero magnetic field $\rho^{xx}$ is given by the inverse of $\sigma^{xx}$ from Eq. (3.13). Unfortunately we do not have an analytic solution of the differential equation Eq. (3.7) for $M_x$, although the coefficients are now known from Eq. (5.1). Numerical integrations of Eqs. (3.7) and (3.13) are performed for different values of $u_0(T)=(1600/T)(\theta_c^2/24)$. For a given value of $\theta_c$, $\rho^{xx}$ is almost precisely linear in $T$ above $T=100$ K (see Fig. 2). The $T=0$ intercept of $\rho^{xx}$, $\rho_0$, is obtained by extrapolating the found high-temperature linear dependence. The RR is defined as $\rho^{xx}(T=100)/\rho_0$, and is typically about 8, say. This is obtained for $u_0(T)\approx 0.022(100/T)$ so that the characteristic small-angle parameter is indeed small, $\theta_c^2/24\approx 0.0014$.

All parameters are now fixed with the exception of $m^*=\hbar k_0/v_0$. The numerical integrations of Eqs. (3.7), (4.6) and (4.8) for $M_y$, $Z$, and $\sigma^{xy}$, respectively, can be carried out for different values of $T$ and combined with the previous result for $\sigma^{xx}(T)$ to give $\cot\theta_H(T)=\sigma^{xx}(T)/\sigma^{xy}(T)$:

$$\cot\theta_H(T)=\frac{0.82}{\omega_c\tau_M}\frac{m^*}{m}\frac{\int d\theta n(\theta)v_x(\theta)M_x(\theta)}{\int d\theta n(\theta)v_x(\theta)Z(\theta)}, \qquad (5.2)$$

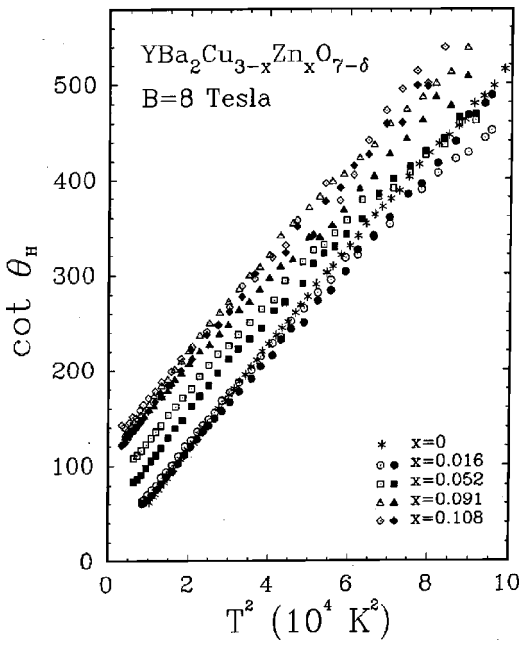


FIG. 3. Data of Chien *et al.* (Ref. 6).

where we have used $\rho=0.54$, $\omega_c$ is the cyclotron frequency with the bare mass, and $n(\theta)=(1-0.54\cos 4\theta)^{-5/4}$.

We now compare our result with the experiment of Chien *et al.*[6] They measured the Hall angle as a function of temperature for various concentrations of Zn impurities in near-optimally doped $YBa_2Cu_3O_{7-\delta}$. Their data at $B=8$ T ($\omega_c=1.28\times 10^{12}$ s$^{-1}$) is reproduced in Fig. 3.

We examine the data for zero Zn concentration. In Fig. 4, we have replotted the $x=0$ points from Fig. 3 (large dots) and the theoretical result (small dots) of Eq. (5.2) with $m^*/m=1.5$, so adjusted to give the best agreement. It is important that $m^*$ turns out to be reasonable. We emphasize that the parameters we picked were determined from ARPES experiments on $Bi_2Sr_2CaCu_2O_{8+\delta}$, while the Hall data is on $YBa_2Cu_3O_{7-\delta}$. Thus, our intent here is only to show that the scattering rates

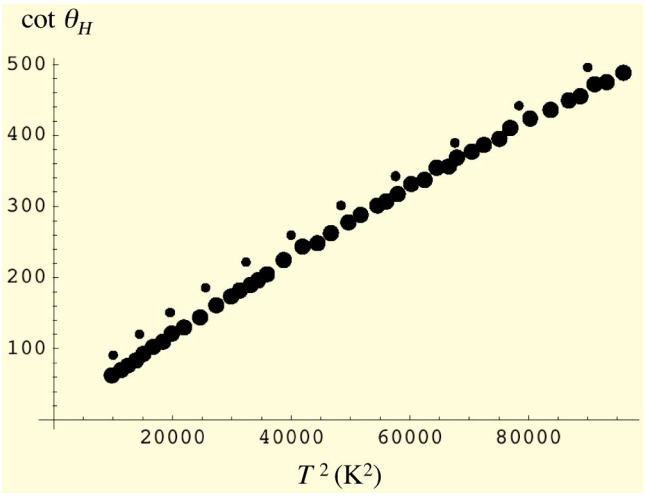


FIG. 4. Theory (small dots) fit to $x=0$ data (large dots) of Chien *et al.* (Ref. 6).

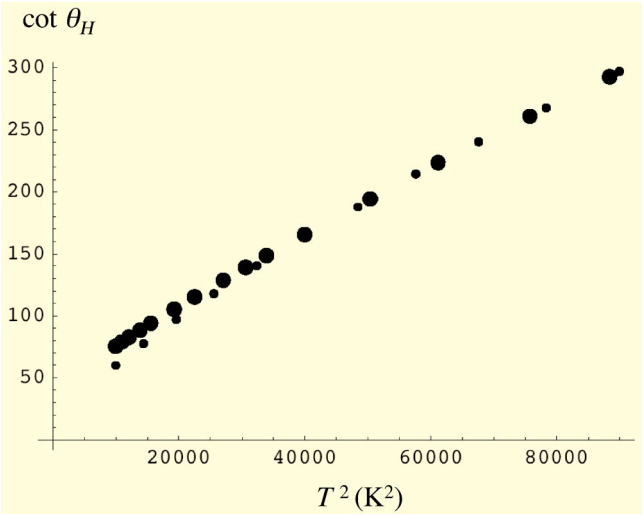


FIG. 5. Comparison of theory (small dots) including in-plane scatterers with data (large dots) from Ref. 9, for optimally doped $Bi_2Sr_{2-x}La_xCuO_6$.

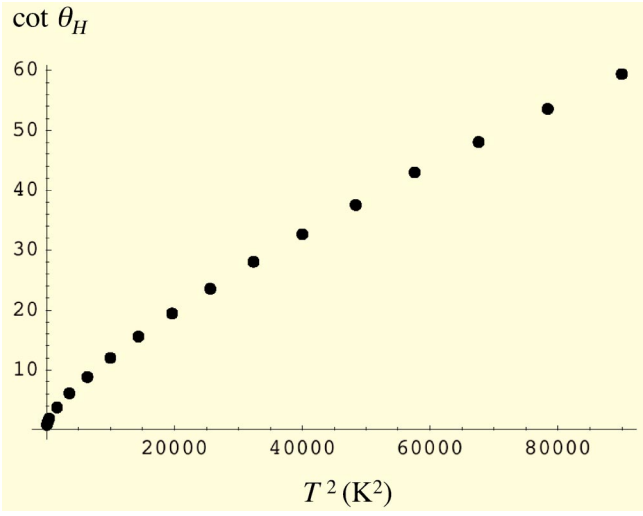


FIG. 6. Theoretical prediction for cot $\theta_H$ down to $T=0$. There is a small intercept at $T=0$ (cot $\theta_H \approx 1.0$) due to in-plane impurity scattering.

characteristic of high-$T_c$ superconductors in the normal state near optimal doping can by themselves account for the temperature dependence of the Hall angle, not to demonstrate quantitative agreement with a particular experiment. It is seen that the experimental temperature dependence is fairly well reproduced.

Notice that the experimental curves have a negative curvature on a $T^2$ plot. While this might suggest a power law less than 2 and several investigators have tried such a fit,[9,10] our picture indicates that this behavior is a consequence of the fact that the conductivities are each the sum of two terms with approximate $1/T^n$ and $1/T^{n+1}$ ($\sigma^{xx}$, $n=1$; $\sigma^{xy}$, $n=2$) dependences.

The data of Ref. 6 and our theory both suggest that in the absence of in-plane impurities such as Zn, the extrapolated cot $\theta_H$ at $T \to 0$ is zero. In-plane impurities will in general not give scattering restricted to small angles. Indeed, their influence is evident in the measured resistivity. We could include their effects by assuming them to be isotropic scatterers that add a constant $1/\tau_z$ to the isotropic linear in temperature MFL rate $1/\tau_M$. This has the effect of an almost parallel upward shift of cot $\theta_H$ so that it has a zero-temperature intercept proportional to $1/\tau_z$, i.e., to the in-plane impurity concentration. We illustrate this qualitatively using some data from Ref. 9. In Fig. 5, we show the data (large dots) for $Bi_2Sr_{2-x}La_xCuO_6$ with $x=0.44$ (optimal doping). It is seen that the data do not extrapolate with a zero intercept. We interpret this as signaling the presence of in-plane scatterers. The theoretical curve (small dots) uses similar parameters as in Fig. 4 but with an in-plane impurity contribution added to $1/\tau_M$.

The availability of very high magnetic fields[18] capable of restoring the normal state below the transition temperature in some cuprate superconductors makes it possible to investigate the Hall effect down to very low temperatures. We conclude this section with our prediction, in Fig. 6, for the behavior of cot $\theta_H$ down to $T=0$ for the case in which the longitudinal resistivity is linear over the whole temperature range. We used the same parameters as in Fig. 5 but the magnetic field was taken to be 50 T, rather than 10 T.

## VI. COMPLEX HALL CONDUCTIVITY

In this section, we comment on the recent ac Hall effect results of Grayson *et al.*[15] For low frequencies and $T > T_c$, we can replace $1\tau_M \approx 1/\tau_{tr}$ by $1/\tau_{tr} - i\omega$. This follows immediately from Eqs. (2.1)–(2.3): the distribution function $g(\mathbf{k},\omega)$ and therefore the transport properties are obtained from the $\omega=0$ results by this replacement.

From Fig. 2 it is seen that the resistivity is almost precisely linear in $T$ in the normal state, $\rho^{xx}=a+bT$, where $a$ is the (small) residual resistivity due to the small-angle impurity scattering. Thus, $a/b$ is about 10, say. We have also found that $\sigma^{xy}(T)$ is, in the temperature range of interest, very closely of the form $c/T^2+d/T^3$, with $c/d \approx 0.01$ K$^{-1}$. Therefore, neglecting quantities of order 0.1, our prediction for the Hall angle is

$$\theta_H(\omega,T) \approx \tan\theta_H = \sigma^{xy}\rho^{xx} \approx A\left[\frac{1}{(1/\tau_{tr}-i\omega)^2}+\frac{c}{d}\frac{1}{(1/\tau_{tr}-i\omega)}\right], \tag{6.1}$$

where $A$ and $c/d$ are constant in temperature. The latter ratio is now in units of seconds; for our example parameters it is about $2\times10^{-14}$ s. We emphasize that a single relaxation rate $1/\tau_{tr}$ enters all our expressions. The constant $A$ in Eq. (6.1) corresponds to the quantity $\omega_H\Omega_p$ of Ref. 15. In that reference, Fig. 4 shows that $A$ is indeed temperature and frequency independent. The $c/d$ term is the conventional term. In Ref. 15, it was shown that by itself it cannot account for the experimental data. Just as the dc data show deviations from $T^2$ behavior for cot $\theta_H$, we expect that the ac data should be fitted by a combination of the two terms in Eq. (6.1). At higher frequencies or temperatures, the conven-

tional term should finally dominate. The complex Hall angle measurements convincingly demonstrate that just one inelastic transport rate determines all the frequency and temperature dependences of the transport properties of the high-$T_c$ superconductors in the marginal Fermi liquid region, i.e., in their normal state near optimum doping.

When calculating the ac conductivity, the limits of applicability of the Boltzmann equation should be kept in mind. The results are only valid for $\omega\tau \ll 1$. In this regime the conservation laws (in terms of bare particles) completely determine transport and the Boltzmann equation deals with them properly. In a microscopic theory, the effects of small-angle scattering calculated here appear as corrections to the coupling of the external magnetic field to the carriers. At high enough frequency these vertex corrections must vanish. The crossover frequency and the behavior of transport properties in the intermediate regime can only be determined by a microscopic calculation. Experimental results at high frequencies do depart from the predictions of Eq. (6.1).

## VII. CONCLUDING REMARKS

Here we discuss sundry issues related to the theory and calculations presented in this paper. We emphasize that this work pertains only to the Hall effect in optimally or overdoped samples. For the latter, the linear-in-temperature scattering rate $1/\tau_M$ should be replaced in the theory by a rate with the $T$ dependence of the observed resistivity. In underdoped cuprates, additional physical considerations appear to determine the transport and equilibrium properties.

### A. Magnetoresistance

Earlier,[5] we gave a plausibility argument that the observed magnetoresistance would follow quantitatively from the same considerations that lead to the observed Hall effect. We leave it as a future exercise to calculate this quantity directly from the solution of the Boltzmann equation as an extension of the present theory.

### B. Small-angle scattering, Fermi surface geometry, bilayer splitting, etc

We have modeled the Fermi velocity through Eq. (3.11), which with $\rho \approx 0.54$ is in itself enough to give the observed angular variation of the elastic part of the single-particle relaxation rate. As we have seen, this also gives agreement with the observed temperature dependence of the Hall angle. This value of $\rho$ is 10% away from the value at which the customary Hall coefficient would be zero. This seems to us reasonable, since in a model with nearest-neighbor Cu-O hopping alone, the Hall effect is zero at half-filling, and with O-O hopping included, the density for zero Hall effect shifts substantially towards hole doping. The optimal doping composition lies in the range 15–20 % hole doping. In this connection, it is important to remember that we are using parameters obtained from experiments on $Bi_2Sr_2CaCu_2O_{8+\delta}$ to fit Hall data on $YBa_2Cu_3O_{7-\delta}$. Therefore the precise numbers are not too meaningful; we only argue that we have shown that the small-angle scattering scenario gives the qualitative features of the experiments.

In our numerical analysis, we have chosen the simplest parametrization of the Fermi velocity to show the plausibility of the small-angle effect in relation to the experiments. Our parametrization should not be expected to represent the Fermi surface adequately. For the actual Fermi surface several terms in Eq. (3.10) for the Fermi velocity would have to be included with coefficients smaller than $\rho$. We note, however, that the successive terms give compensatingly larger coefficients since the higher harmonics produce larger derivative terms in Eq. (5.2) for $\sigma_{xy}$. For a truer Fermi surface the advantage of analytical calculations is lost. These remarks are of academic interest at the present time since the actual Fermi surface is not accurately known.

More relevant is the fact that the Fermi surface of $Bi_2Sr_2CaCu_2O_{8+\delta}$, the ARPES data for which we have used here, has two sheets coming from the bilayer splitting. The bilayer splitting varies as a function of angle, being largest in the $(\pi,0)$ direction. This arises because of the geometry of the interlayer orbitals.[19] This angular variation is essentially the same as that of the observed anisotropic elastic scattering. The fact that the bilayer splitting is not resolved in the experimental data we have used indicates the presence of an elastic scattering mechanism that couples the layers. We surmise that for interlayer or intralayer scattering due to impurities between the planes, the same orbitals are involved and therefore the same angular dependence arises in scattering. In a single-layer model as treated here, this effect is parametrized through the choice of the angle dependence of the Fermi velocity as in Eq. (3.11).

### C. Comments on related work

As already remarked, although the analytical expressions derived in our earlier work[5] are correct, we erred, as pointed out by Yakovenko,[13] in our choice of the parametrization in which they were evaluated. This error has been remedied here. Our more complete analysis with a simpler parametrization in fact gives results consistent with experiment. We have shown that not only do we get the right temperature dependence but that with a reasonable effective mass, the absolute value of the cotangent of the Hall angle is obtained within 10% of the data from the same parametrization.

In Ref. 20, Hlubina argues that the term discovered by us, if adequate to explain the Hall angle, would make an unacceptable contribution to the longitudinal resistivity. Since our parameters are actually determined by the measured resistivity, this criticism is invalid. It is difficult to make a direct comparison with the calculations of Ref. 20 since a quite different parametrization of the Fermi surface is used there. However, we can note that the parametrization family used in Hlubina's evaluation does not include ours and gives a much larger conventional contribution to $\sigma^{xy}$ than the one we have used.

A recent paper of Carter and Schofield[21] addresses the main point of our original paper.[5] Their work consists of two parts. One is analytical, the other is a numerical solution of

equations we derived in Ref. 5. We cannot comment on the adequacy of the numerical work, but Carter and Schofield are indeed correct that the customary term (with a different temperature dependence than our term) is zero only for a particular choice of Fermi surface. This is of course well known: the traditional Hall angle is zero only for ''particle-hole symmetry'' defined in terms of the curvature of the Fermi surface. However, as we have shown here, it is not necessary that the customary term be zero (and all the temperature dependence come from our term) to get good agreement with experiment. It is sufficient that the customary term is about a factor of 4 smaller than our term at $T \approx 100$ K. In fact, the experimental data for $\cot \theta_H$, when plotted against $T^2$, usually shows a slight downward curvature. This point has been discussed in Sec. I and is adequately demonstrated in the experimental data shown in Figs. 3–5.

The analytical calculation of Ref. 21, expressed in their Eqs. (7)–(10), is not sufficiently general to contain the anisotropies required to show the effect we have derived. Their calculation for $\sigma^{xy}$ is equivalent to retaining only the impurity scattering contribution to the conventional term, not the contribution that we have derived. See Footnote 22 of Ref. 21 for a comment on this. Actually, the analytical calculation of Ref. 21 is based on a circular Fermi surface and we agree that such a parametrization never leads to a large enough effect.

## ACKNOWLEDGMENTS

We thank V. Yakovenko, D. Drew, and M. Grayson for helpful discussions of our analysis and A.J. Schofield for informative communications. N.P. Ong and Y. Ando generously provided experimental data. E.A. was supported in part by NSF Grant No. DMR99-76665. The authors acknowledge the hospitality of the Aspen Center for Physics where part of this work was carried out.

[1] C.M. Varma, P.B. Littlewood, S. Schmitt-Rink, E. Abrahams, and A.E. Ruckenstein, Phys. Rev. Lett. **63**, 1996 (1989).

[2] F. Slakey, M.V. Klein, J.P. Rice, and D.M. Ginsberg, Phys. Rev. B **43**, 376 (1991).

[3] T. Valla, A.V. Fedorov, P.D. Johnson, B.O. Wells, S.L. Hulbert, Q. Li, G.D. Gu, and N. Koshizuka, Science **285**, 2110 (1999); A.V. Fedorov, P.D. Johnson, Q. Li, G.D. Gu, and N. Koshizuka, Phys. Rev. Lett. **85**, 828 (2000); A. Kaminsky, J. Mesot, H. Fretwell, J.C. Campuzano, M.R. Norman, M. Randeria, H. Ding, T. Sato, T. Takahashi, T. Mochiku, K. Kadowaki, and H. Hoechst, *ibid.* **84**, 1788 (2000); A. Kaminsky and J.C. Campuzano (private communication) (some of the pertinent data is reproduced in Ref. 4).

[4] Elihu Abrahams and C.M. Varma, Proc. Natl. Acad. Sci. U.S.A. **97**, 5714 (2000).

[5] C.M. Varma and Elihu Abrahams, Phys. Rev. Lett. **86**, 4652 (2001).

[6] T.R. Chien, Z.Z. Wang, and N.P. Ong, Phys. Rev. Lett. **67**, 2088 (1994).

[7] J.M. Harris, Y.F. Yan, and N.P. Ong, Phys. Rev. B **46**, 14 293 (1992); Phys. Rev. Lett. **75**, 1391 (1996); A. Carrington, A.P. Mackenzie, C.T. Lin, and J.R. Cooper, *ibid.* **69**, 2855 (1992).

[8] H.Y. Hwang, B. Batlogg, H. Takagi, H.L. Kao, J. Kwo, R.J. Cava, J.J. Krajewski, and W.F. Peck, Jr., Phys. Rev. Lett. **72**, 2636 (1994).

[9] Yoichi Ando and T. Murayama, Phys. Rev. B **60**, 6991 (1999).

[10] Z. Konstantinovć, Z.Z. Li, and H. Raffy, Phys. Rev. B **62**, 11 989 (2000).

[11] H.D. Drew, S. Wu, and H.-T.S. Lihn, J. Phys.: Condens. Matter **8**, 10037 (1996).

[12] See Eqs. (23) and (24) of Ref. 1.

[13] V. Yakovenko (private communication).

[14] C.M. Varma and Elihu Abrahams, Phys. Rev. Lett. **88**, 139903(E) (2002).

[15] M. Grayson, L.B. Rigal, D.C. Schmadel, H.D. Drew, and P.-J. Kung, Phys. Rev. Lett. **89**, 037003 (2002).

[16] R. Hlubina has pointed out the failure of the relaxation time approximation in the case of forward scattering: Phys. Rev. B **62**, 11 365 (2000).

[17] G. Kotliar, A.M. Sengupta, and C.M. Varma, Phys. Rev. B **53**, 3573 (1996).

[18] See, for example, S. Ono, Yoichi Ando, T. Murayama, F.F. Balakirev, J.B. Betts, and G.S. Boebinger, Phys. Rev. Lett. **85**, 638 (2000).

[19] S. Chakravarty, A. Sudbø, P.W. Anderson, and S. Strong, Science **261**, 337 (1993); O.K. Andersen, A.I. Liechtenstein, O. Jepson, and F. Paulson, J. Phys. Chem. Solids **56**, 1573 (1995).

[20] R. Hlubina, Phys. Rev. B **64**, 132508 (2001).

[21] E.C. Carter and A.J. Schofield, Phys. Rev. B **66**, 241102(R) (2002).